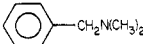
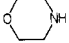
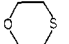


Table V. Free-Energy Difference, ($\Delta\Delta G^\ddagger$ at 30 °C) for Additions and Retroadditions to the 4a-Positions of C^1 - Fl_{ox}^+Et and Fl_{ox}^+Et and for Oxidations by C^1 -4a- $FlEtOOH$ and 4a- $FlEtOOH$

4a-pseudobase formation ($\Delta G^\ddagger_{C^1} - \Delta G^\ddagger_{N^1} = \Delta\Delta G^\ddagger$, kJ M ⁻¹)	
k_0, s^{-1}	2.8
$k_1, M^{-1} s^{-1}$	0.5
$k_2, M^{-1} s^{-1}$	4.5
H ₂ O solvent	
4a-thiol addition	
k_f, s^{-1}	2.6
k_r, s^{-1}	3.8
oxidations (M ⁻¹ s ⁻¹) of	
I ⁻	3.0 95% EtOH
	6.1
	7.1
	7.1
DMF	
4a-peroxide dissociation	
k_1, s^{-1}	6.7

^a The k_0 values have been extrapolated to zero buffer concentration.

Inspection of Table V reveals that with a particular solvent, the values of $\Delta\Delta G^\ddagger$ ($=\Delta G^\ddagger_{C^1} - \Delta G^\ddagger_{N^1}$) are similar for the reactions investigated (save the acid-catalyzed process associated with k_1 of pseudobase formation). This observation supports a greater electrophilicity of the 4a-position of the N^1 flavins when compared to the C^1 flavins and a greater polarization of the peroxide moiety

of the N^1 -4a- $FlEtOOH$ as compared to C^1 -4a- $FlEtOOH$. Inspection of Table V also shows that the dissociation rate constants (for RS^- , HO^- , and HOO^-) from the 4a-position of the N^1 flavin are larger than those seen with the C^1 flavin. The ground states of C^1 - Fl_{ox}^+Et and Fl_{ox}^+Et differ in free energy content by the same amount as the ground states of the products C^1 -4a- $FlEtX$ and 4a- $FlEtX$. Lowering of the free-energy content of the transition state for addition of X must also lower the ground state for dissociation of X and by the same value of $\Delta\Delta G^\ddagger$. Particularly noteworthy from Table V is the similarity of the $\Delta\Delta G^\ddagger$ for the N- and S-oxidation reactions in DMF to the $\Delta\Delta G^\ddagger$ for dissociation of peroxide from the C^1 and N^1 flavin hydroperoxides in that same solvent. Evidently the difference in polarization about the C_{4a} -OOH bond in 4a- $FlEtOOH$ relative to C^1 -4a- $FlEtOOH$ is reflected in the difference in polarization about the C_{4a} O-OH bond and in facilitation of the N- and S-oxidation reactions.

From the present study, it is concluded that 1-carba-1-deaza FAD should, if recognized by the enzyme, serve as a cofactor for the hepatic flavoprotein microsomal oxidase in the N-oxidation of amines and the S-oxidation of sulfides.

Acknowledgment. This work was supported by grants from the National Institutes of Health and the National Science Foundation. We should like to acknowledge the experimental contribution of Mr. Thomas Malefyt. It is our pleasure to acknowledge the gifts of comparison samples of various carbade-azafavins which have been provided to us in recent years by Dr's. E. F. Rogers and W. T. Ashton of Merck Sharp and Dohme Research Laboratories, Rahway, N.J. We are also grateful to these gentlemen for their sharing with us of various synthetic observations prior to their publication.

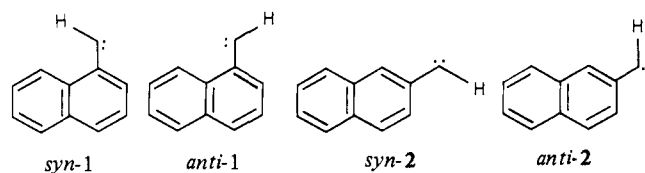
Conformational Barriers in Triplet 1- and 2-Naphthylcarbene. 2. Absolute Rate of Decay of Arylcarbenes by Electron Spin Resonance Spectroscopy

V. P. Senthilnathan¹ and Matthew S. Platz*

Contribution from the Department of Chemistry, The Ohio State University, Columbus, Ohio 43210. Received November 17, 1980

Abstract: The absolute decay of the syn and anti forms of 1- and 2-naphthylcarbene and 9-anthryl- and 2-pyrylcarbene have been measured at low temperature by ESR. The decay rates are pseudo first order and arise from reaction of the carbene with the crystalline host. The signal decay is nonexponential due to site problems in the matrix. The decay can be fitted to a $\log I$ vs. $t^{1/3}$ dependence. Matrix isotope effects reveal that the mechanism of carbene decay is by abstraction of hydrogen atom from the matrix by tunneling through a small barrier. The kinetics reveal that equilibration of the syn and anti forms of 1- and 2-naphthylcarbene is much slower than their reaction with the matrix. The activation barrier to syn-anti interconversion must be greater than 4.5-6.3 kcal/mol.

In 1965 Trozzolo et al. observed two distinct sets of triplet electron spin resonance (ESR) spectra in the low-temperature photolysis of 1- and 2-naphthyldiazomethane.² The spectra were assigned to the syn and anti forms of the matrix-isolated carbenes **1** and **2**. 9-Anthrylcarbene **3**, which has two equivalent planar

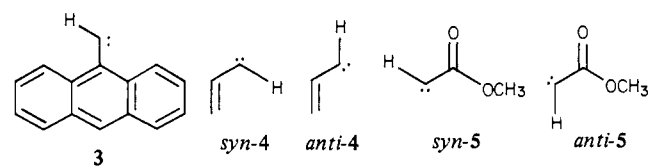


forms, gives only a single spectrum. These observations confirmed

(1) Department of Chemistry, P.S.G. Arts and Sciences College, Coimbatore-641014, India.

(2) Trozzolo, A. M.; Wasserman, E.; Yager, W. A. *J. Am. Chem. Soc.* **1965**, *87*, 129-130.

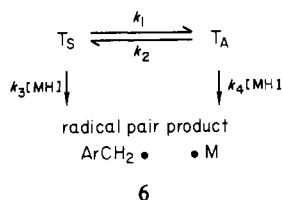
previous theoretical and experimental observations that arylcarbenes are nonlinear.³ Geometric isomerism in triplets has been observed subsequently in vinylcarbene **4** and carbomethoxy-carbene⁴ **5**. Interconversion of the two triplet forms may occur



(3) (a) Foster, J. M.; Boys, S. F. *Rev. Mod. Phys.* **1960**, *32*, 305; (b) Wasserman, E.; Trozzolo, A. M.; Yager, W. A.; Murray, R. W. *J. Chem. Phys.* **1964**, *40*, 2408.

(4) (a) Hutton, R. S.; Manion, M. L.; Roth, H. D.; Wasserman, E. *J. Am. Chem. Soc.* **1974**, *96*, 4680-4681; (b) Hutton, R. S.; Roth, H. D. **1978**, *100*, 4324-4325.

Scheme 1



via out-of-plane rotation or by linearization through an sp-hybridized center. The mechanism and barrier to the interconversion has not been established by direct experiment as the carbenes do not survive the high temperatures necessary to coalesce the spectra. Recently, Schaeffer⁵ has calculated a barrier of 4.93 kcal/mol to rotation in **5**.

We have recently shown that the rate of bimolecular reactions of diarylcarbenes in viscous organic media can be monitored by ESR.⁶ Experimentally, one irradiates a precooled sample of aryldiazo compound in a polycrystalline or glassy organic matrix in the probe of an ESR spectrometer. This produces a metastable sample of triplet carbene which is monitored by its magnetic resonance absorption. The absolute rate of decay of the triplet carbene ESR signal is measured by ceasing sample irradiation and scanning the absorption peak as a function of time. That the decay of the triplet ESR signal is due to reaction of the diarylcarbene with the matrix has been demonstrated by analysis of the reaction products and by kinetic arguments. Our previous work indicated that there are several differences between solution⁷ and matrix kinetics of triplet arylcarbenes. At low temperature the triplet decay of diarylcarbenes occurs by quantum mechanical tunneling of hydrogen atoms through a small barrier.⁶

The bimolecular decay kinetics of 1- and 2-naphthylcarbene are characterized by four rate constants. This is shown in Scheme 1, where T_S and T_A are the syn and anti forms of the respective carbene conformers, and MH is the solvent matrix.

There are only two measurable experimental quantities, the decay rate of T_S and T_A , $-dT_S/dt = k_{syn}[T_S]$ and $-dT_A/dt = k_{anti}[T_A]$. A complete kinetic analysis is therefore impossible, but consideration of two extreme cases is informative.

Case A. Slow Equilibration. If equilibration of T_S and T_A is much slower than their bimolecular reactions, they will decay independently. That is $k_3[MH] \gg k_1$ and $-dT_S/dt = k_3[T_S][MH]$; $k_4[MH] \gg k_2$ and $-dT_A/dt = k_4[T_A][MH]$. If $-dT_S/dt \neq -dT_A/dt$, the rate of each carbene reaction with the matrix must be at least comparable to, if not much greater than, the rate of equilibration.

Case B. Rapid Equilibration. If equilibration of T_S and T_A is much faster than their bimolecular reactions, the two carbenes will decay at the same rate, $-dT_S/dt = -dT_A/dt$. The relative amounts of T_S and T_A will reflect the equilibrium constant K .

$$K = \frac{[T_S]}{[T_A]} = \exp \left[\frac{E_{T_A} - E_{T_S}}{RT} \right]$$

Experimentally, the observation that $-dT_S/dt = -dT_A/dt$ is a necessary but insufficient condition of case B.⁸ Case A may be operative, but fortuitously $k_3 = k_4$.

Results and Discussion

In a footnote to their paper, Trozzolo et al. mentioned that both sets of triplet signals of **1** and **2** could not be observed in every matrix at 77 K due to unstable signals.² We have also found this to be the case. The D_{ZZ} signals observed from 1-naphthylcarbene

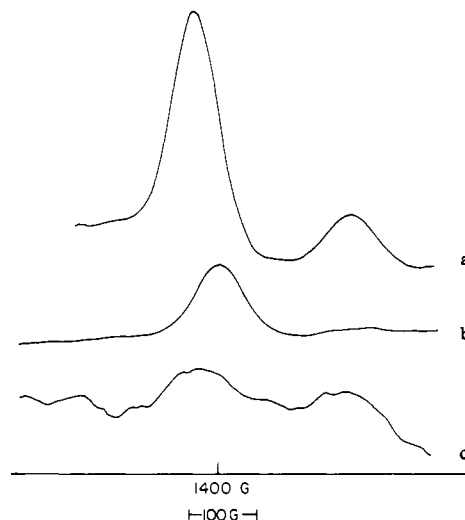


Figure 1. The D_{ZZ} transitions of the triplet syn (low field) and anti (high field) forms of 1-naphthylcarbene in (a) 2-propanol, (b) 2MTHF, and (c) benzene.

at 77 K in several hosts are shown in Figure 1. In most solvents the syn-1-naphthylcarbene peak is much more intense than the anti form. The anti form **1A** is not observed in 2-methyltetrahydrofuran (2MTHF), but both **1A** and **1S** are equally intense in benzene. If the conditions of case A are operative throughout the series, the relative peak intensities reflect the rate of formation and decay of the two triplet conformers as a function of solvent. If the scenario of case B prevails, the relative peak intensities reflect the variation of syn-anti equilibrium constant with matrix. These interpretations will be distinguished in a later section.

ESR spectroscopy has been used by several groups to follow the decay of free radicals in solids and glasses at low temperature. Despite the fact that the radical decay is pseudo first order, simple-first-order kinetics are not always observed.⁹ This has been explained as a multiple-site problem.¹⁰ The free radicals are not generated homogeneously in the viscous medium. They are immobilized relative to the host molecules with which they react. Different fixed orientations of the radical relative to the host produce different rate constants and deviate from simple-first-order kinetics.

The decay of the ESR signal intensities (I) of **1A**, **1S**, **2A**, **2S**, and **3** are not simple first order. Characteristically, a plot of $\log I$ vs. time (t) significantly deviates from linearity even at short reaction time. However, a plot of $\log I$ vs. $t^{1/3}$ is linear up to at least 80% of the signal decay in polycrystalline matrices.

Unusual kinetic orders of this type have been observed previously. Bol'Shakov has found that the decay of methyl radical in methanol-water glasses is best fit by a $t^{1/2}$ dependence.¹¹ Our previous work on diarylcarbenes indicated that $t^{1/2}$ works well in glasses but $t^{1/3}$ should be employed for decay in polycrystals.⁶ This unusual carbene kinetic order has been confirmed by Gaspar.¹² The non first-order decay of matrix-isolated triplet carbenes is completely analogous to that observed with free radicals. The explanation is identical: different fixed orientations of the carbene in the matrix lead to different rate constants and non first-order behavior. The unusual $t^{1/2}$ kinetic order has been explained by Bol'Shakov by a quantum mechanical argument.¹¹ It may also be possible to explain the results by using a statistical model which encompasses the variation of the rate constant within the matrix.¹³

(9) (a) Sprague, E. D. *J. Phys. Chem.* **1973**, *77*, 2066-2070; (b) Neiss, M. A.; Willard, J. E. *Ibid.* **1975**, *79*, 783-791; (c) Neiss, M. A.; Sprague, E. D.; Willard, J. E. *Ibid.* **1972**, *76*, 546-1121; (d) French, W. A.; Willard, J. E. *Ibid.* **1968**, *72*, 4604-4608.

(10) Hudson, R. L.; Shiotan, M.; Williams, F. *Chem. Phys. Lett.* **1977**, *48*, 193-195.

(11) (a) Bol'Shakov, Z. V.; Tolkatchen, V. A. *Chem. Phys. Lett.* **1976**, *40*, 468-470. (b) Bol'Shakov, Z. V.; Fuks, M. P.; Tolkatchev, V. A.; Burstein, A. I. *Radiat. Chem. 4th* **1976**, *4*, 723-725.

(12) Line, C. T.; Gaspar, P. P. *Tetrahedron Lett.* **1980**, 3553-3556.

(5) Kim, K. S.; Schaefer, H. F. III *J. Am. Chem. Soc.* **1980**, *102*, 5389-5390.

(6) Senthilnathan, V. P.; Platz, M. S. *J. Am. Chem. Soc.* **1980**, *102*, 7637-7643.

(7) (a) Closs, G. L.; Rabinow, B. E. *J. Am. Chem. Soc.* **1976**, *98*, 8190-8198; (b) Zupancic, J. J.; Schuster, G. B. *Ibid.* **1980**, *102*, 5958-5960.

(8) We thank Dr. H. D. Roth for useful discussions.

Table I. Pseudo-First-Order Matrix Rate Constants for 1-Naphthylcarbene

matrix	temp, °C	$k_{\text{syn}}, \text{s}^{-1/3}, 1300 \text{ G}$	$k_{\text{anti}}, \text{s}^{-1/3}, 1500 \text{ G}$	$k_{\text{anti}}/k_{\text{syn}}$	concn, M
2-PrOH	-196	0.105 ± 0.004	0.172 ± 0.012	1.64	s ^a
	-186	0.133 ± 0.012			s
	-178	0.196 ± 0.016			s
2-PrOH- <i>O-d</i>	-196	0.099 ± 0.006	0.186 ± 0.010	1.88	s
	-185	0.137 ± 0.012			s
	-181	0.194 ± 0.018			s
(CH ₃) ₂ COH(D)	-196	0.067 ± 0.004	0.115 ± 0.008	1.70	s
	-185	0.109 ± 0.006			s
	-181	0.158 ± 0.008			s
(CD ₃) ₂ COH(H)	-196	0.057 ± 0.003	0.091 ± 0.005	1.58	s
	-181	0.141 ± 0.010			s
	-177	0.179 ± 0.006			s
<i>i</i> -PrOH- <i>d</i> ₈	-196	0.031 ± 0.002	0.040 ± 0.003	1.25	s
	-181	0.089 ± 0.008			s
	-177	0.139 ± 0.006			s
toluene	-196	0.127 ± 0.004	0.141 ± 0.016	1.11	0.173
	-184	0.184 ± 0.006			0.173
	-182	0.246 ± 0.024			0.173
toluene- <i>d</i> ₈	-196	0.034 ± 0.002	0.045 ± 0.040	1.34	0.167
	-182	0.091 ± 0.010			0.93
	-178	0.141 ± 0.006			1.07

^a Saturated (<0.1 M).

Table II. Pseudo-First-Order Matrix Rate Constants for 2-Naphthylcarbene

matrix	temp, °C	$k_{\text{syn}}, \text{s}^{-1/3}, 1600 \text{ G}$	$k_{\text{anti}}, \text{s}^{-1/3}, 2000 \text{ G}$	$k_{\text{syn}}/k_{\text{anti}}$	concn, M
2-PrOH	-196	0.057 ± 0.004	0.061 ± 0.008	0.93	s ^a
	-184		0.105 ± 0.008		s
	-182		0.135 ± 0.004		s
2-PrOH- <i>d</i> ₈	-196	0.035 ± 0.0016	0.026 ± 0.004	1.38	s
	-182		0.063 ± 0.006		s
	-176		0.067 ± 0.004		s
2-PrOH-2- <i>d</i> ₁	-196	0.085 ± 0.004	0.067 ± 0.002	1.27	s
	-179		0.117 ± 0.004		s
	-182		0.147 ± 0.002		s
2-PrOH- <i>O-d</i>	-196	0.095 ± 0.006	0.081 ± 0.004	1.17	s
	-184		0.166 ± 0.006		s
	-182		0.184 ± 0.008		s
toluene	-196	0.101 ± 0.004	0.115 ± 0.004	0.88	0.116
	-182		0.158 ± 0.002		0.116
	-185		0.180 ± 0.010		0.116
toluene- <i>d</i> ₈	-196	0.055 ± 0.006	0.030 ± 0.006	1.86	0.1
	-183		0.071 ± 0.006		1.50
	-180		0.095 ± 0.007		0.1

^a Saturated (<0.1 M).

A $t^{1/2}$ kinetic dependence is frequently observed in energy transfer reactions. The rate of energy transfer from a donor molecule (D*) to an acceptor (A) is critically dependent upon their separation (r). When (r) is small the rate of energy transfer between the nearby D* and A molecules is rapid. At large separations the energy transfer rate constant is much smaller. If the sample contains a uniform distribution of distances r , between the reacting partners, a $t^{1/2}$ kinetic order can be derived. This circumstance is known as Förster transfer or Förster kinetics.¹⁴

The pseudo-first-order matrix decay rate constants of 1-naphthylcarbene are listed in Table I. Each rate constant is the average of three determinations measured up to 50–70% of the signal decay. The rate constants are reported in units of $\text{s}^{-1/3}$ and their reproducibility is generally better than ±5%. The data for 2-naphthylcarbene are reported in Table II.

It is possible to obtain initial pseudo-first-order rate constants for 1- and 2-naphthylcarbene by examining only the first 20% of the decay reaction. In this method we are selecting only a small portion of all of the reactive matrix sites for analysis. The fixed

Table III. Pseudo-First-Order Initial Rate Constants for 1-Naphthylcarbene (±20%) at 77 K

matrix	$k_{\text{syn}}, \text{s}^{-1}, 1300 \text{ G}$	$k_{\text{anti}}, \text{s}^{-1}, 1600 \text{ G}$	$k_{\text{anti}}/k_{\text{syn}}$
2-PrOH	0.001 50	0.003 23	2.08
2-PrOH- <i>O-d</i>	0.001 60	0.002 05	1.30
2-PrOH-2- <i>d</i>	0.000 70	0.001 43	2.05
CD ₃ CHOHCD ₃	0.000 57	0.001 65	2.90
2-PrOH- <i>d</i> ₈	0.000 18	0.000 43	2.35
toluene	0.001 55	0.001 68	1.08
toluene- <i>d</i> ₈	0.000 27	0.000 25	0.91

Table IV. Pseudo-First-Order Initial Rate Constants for 2-Naphthylcarbene (±20%) at 77 K

matrix	$k_{\text{syn}}, \text{s}^{-1}, 1600 \text{ G}$	$k_{\text{anti}}, \text{s}^{-1}, 2000 \text{ G}$	$k_{\text{anti}}/k_{\text{syn}}$
2-PrOH	0.001 10	0.000 50	0.46
2-PrOH-2- <i>d</i>	0.001 01	0.000 90	0.90
2-PrOH- <i>O-d</i>	0.001 16	0.001 16	1.00
2-PrOH- <i>d</i> ₈	0.000 13	0.000 12	0.90
toluene	0.001 55	0.001 81	1.16
toluene- <i>d</i> ₈	0.000 31	0.000 13	0.42

orientation of the carbenes in the selected sites must be similar and have roughly the same pseudo-first-order rate constants. By

(13) Professor Jack Hine has found that a plot of $\log(I)$ vs. $t^{1/2}$ plot will be linear ($R > 0.99$) if one assumes a Gaussian distribution of rate constants within the matrix and there is a 10^3 fold range of rate constants within four standard deviations of the most probable rate constant.

(14) J. J. Yardley "Introduction to Molecular Energy Transfer"; Academic Press: New York, 1980; pp 234–241.

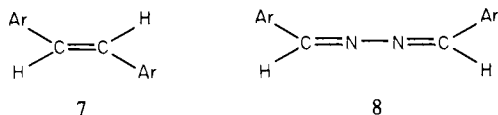
Table V. Matrix Arrhenius Parameters for Bimolecular Rate Decay of *syn*-1-Naphthylcarbene

	$\log A, \text{s}^{-1/3} \text{M}^{-1}$	$E, \text{cal/mol}$
2-PrOH	-0.5 ± 0.14	533 ± 40
2-PrOH- <i>O-d</i>	-0.2 ± 0.29	642 ± 106
2-PrOH-2- <i>d</i>	0.1 ± 0.21	810 ± 86
2-PrOH- <i>d</i> ₈	0.2 ± 0.22	881 ± 66
2-PrOH- <i>d</i> ₈	0.74 ± 0.22	1141 ± 100
toluene	-0.12 ± 0.21	655 ± 78
toluene- <i>d</i> ₈	0.64 ± 0.20	1151 ± 95

choosing the initial 20% of decay, we are analyzing the most reactive sites observable in the matrix. This method allows us to discuss a small portion of the matrix kinetics in terms of pseudo-first-order solution kinetics. These rate constants are reported in Tables III and IV in units of s^{-1} . The initial rate constants are much less precise than the matrix rate data. The $\text{s}^{-1/3}$ unit is larger than the s^{-1} ; hence the variation in rate constants is artificially much smaller in the former scale. Unless otherwise specified, we will be referring to matrix rate constants in future discussions.

Inspection of Table I reveals that anti-1 is more reactive than *syn*-1 at 77 K. The ratio of $k_{\text{anti}}/k_{\text{syn}}$ approaches 2 at this temperature. At higher temperatures it was not always possible to measure k_{anti} . At those elevated temperatures where both values could be determined, a reversal in relative reactivity was observed: $k_{\text{syn}} > k_{\text{anti}}$. As $k_{\text{syn}} \neq k_{\text{anti}}$ in seven matrices at 77 K the fast equilibrium scenario (case B) can immediately be ruled out of consideration for 1-naphthylcarbene. The data of Table II indicate that $k_{\text{syn}} \approx k_{\text{anti}}$ for 2-naphthylcarbene in 2-propanol and toluene at 77 K. This is consistent with case B (fast equilibrium) but does not prove its existence in these solvents.

Solvent Kinetic Isotope Effects. The study of solvent kinetic isotope effects can be richly rewarding in several regards. Firstly, it is not immediately apparent from the rate studies what specific reaction is responsible for the decay of the carbene. The triplet carbenes may react with themselves to give dimer 7, or diazo precursor to give azine 8, or with the matrix to give a radical pair 6. Although product studies of several matrix-isolated aryl-



carbenes show that very little 7 or 8 is formed,¹⁵ this does not a priori rule out the involvement of these processes in the observed kinetics. Due to the high sensitivity of ESR spectroscopy, one might be focusing on a minor chemical process. Isotopic substitution of the solvent will produce a large primary effect if one is following the rate of hydrogen abstraction from the matrix. A similar rate retardation is not expected for dimerization or for azine formation. The data of Tables I and II show significant rate retardation upon isotopic substitution of the matrix. This is most consistent with hydrogen atom abstraction as the mechanism of carbene decay, and it is consistent with previous work on diphenylcarbene and fluorenylidene.⁶

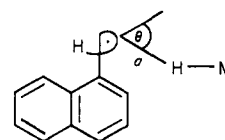
The Arrhenius parameters of 1- and 2-naphthylcarbene are listed in Tables V and VI. To obtain the data one must convert the pseudo-first-order rate constants of Tables I and II to true-second-order rate constants by dividing the former by $[\text{MH}]$. The matrix concentration is not known precisely due to the contraction of the solvent upon cooling. For our purposes we will assume $[\text{MH}] = 10 \text{ M}$ for each matrix, although this introduces some

Table VI. Matrix Arrhenius Parameters for Bimolecular Rate Decay of *anti*-2-Naphthylcarbene

	$\log A, \text{s}^{-1/3} \text{M}^{-1}$	$E, \text{cal/mol}$
2-PrOH	-0.55 ± 0.13	575 ± 46
2-PrOH- <i>O-d</i>	-0.08 ± 0.22	711 ± 82
2-PrOH-2- <i>d</i>	-0.27 ± 0.19	683 ± 45
2-PrOH- <i>d</i> ₈	-0.10 ± 0.27	868 ± 103
toluene	-0.35 ± 0.20	596 ± 73
toluene- <i>d</i> ₈	0.18 ± 0.29	968 ± 117

imprecision into the Arrhenius data. The Arrhenius parameters also suffer from the limited temperature range available for study ($\approx 20 \text{ K}$). For these reasons one should not attach much quantitative significance to the Arrhenius data. However, the parameters are very revealing qualitatively. The parameters are much smaller than anticipated for a solution reaction; $\log A$ varies from -1 to $2 \text{ M}^{-1} \text{ s}^{-1/3}$, E_a is in the range of 500 – 1500 cal/mol . This is not a consequence of using matrix rate constants in units of $\text{s}^{-1/2}$ or $\text{s}^{-1/3}$. The use of initial rate constants, which are a closer analogue to true solution rate constants ($20\% \text{ decay, s}^{-1}$), leads to qualitatively the same Arrhenius data.⁶ The solvent isotope effects are particularly revealing. Isotopic substitution of the solvent invariably and dramatically increases both $\log A$ and E_a . The data requires that the hydrogen atom transfer from the solvent is not a classical process but proceeds instead via quantum mechanical tunneling of a hydrogen atom through a small barrier.¹⁶ The interpretation is identical with that previously presented for diarylcarbenes⁶ and the pioneering work of Williams with matrix-isolated methyl radical.¹⁷

The wide variation of rate constants among the reactive sites in the matrix is easily explained by a tunneling mechanism. The tunneling rate constant is a sensitive function of barrier height and width in all theoretical models.¹⁸ The barrier width is the distance, a , the hydrogen atom must tunnel, and the barrier height is the classical activation energy. Small variations in a and θ



will affect the barrier width and height and have a substantial effect on the tunneling rate constant.¹⁹

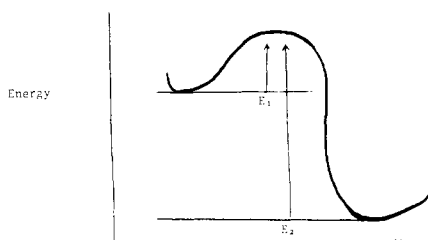
The matrix isotope effects can also be used to distinguish slow or fast equilibration of the carbene conformers. If the carbene decay could be slowed while the rate of equilibration remained unchanged, the decay mechanism might change from case A to that of case B. This is just the anticipated effect of isotopic matrix substitution. The matrix isotope effect on the equilibration process should be minor, and as previously discussed, there are large isotope effects on the decay processes due to tunneling. The change in $k_{\text{anti}}/k_{\text{syn}}$ with isotopic composition of the matrix is given in Tables I and II for 1- and 2-naphthylcarbene on passing from 2-propanol to 2-propanol-*d*₈. It is tempting to interpret this change as an approach to fast equilibrium conditions, but there are several problems with this reasoning. First, the $k_{\text{anti}}/k_{\text{syn}}$ ratio actually increases in 2-propanol-*O-d* and 2-propanol-2-*d* relative to 2-propanol. The $k_{\text{anti}}/k_{\text{syn}}$ ratio of 1-naphthylcarbene also increases on passing from toluene to toluene-*d*₈. The simplest explanation is that both the *syn* and *anti* forms of 1-naphthylcarbene have

(16) Caldin, E. F. *Chem. Rev.* **1969**, *39*, 135–156.(17) Campion, A. and Williams, F. *J. Am. Chem. Soc.* **1972**, *94*, 7633–7637; see also ref 18. (b) Wang, J. T.; Williams, F. *Ibid.* **1972**, *94*, 2930–2934; (c) Le Roy, R. J.; Sprague, E. D.; Williams, F. *J. Phys. Chem.* **1972**, *76*, 564–551.

(18) Bell, R. P. "The Tunnel Effect in Chemistry"; Chapman and Hall: New York, 1980.

(19) Professor C. W. McCurdy has performed preliminary tunneling calculations which indicate that a change of 0.5 \AA in barrier width or 2 kcal/mol barrier height changes the tunneling rate constant by orders of magnitude.(15) (a) Moss, R. A.; Joyce, *J. Am. Chem. Soc.* **1978**, *100*, 4475–4480; (b) Moss, R. A.; Huselton, J. K. *Ibid.* **1978**, *100*, 1314–1315; (c) Moss, R. A.; Joyce, M. A. *Ibid.* **1977**, *99*, 1262–1264; (d) Moss, R. A.; Dolling, U. H. *Ibid.* **1971**, *93*, 954–960; (e) Tomioka, H.; Griffin, G. W.; Nishiyama, K. *Ibid.* **1979**, *100*, 6009–6012. (f) Tomioka, H.; Inagaki, T.; Nakamura, S.; Izawa, Y. *J. Chem. Soc., Perkin Trans. 1* **1979**, 130–134; (g) Tomioka, H.; Izawa, Y. *J. Am. Chem. Soc.* **1977**, *99*, 6128–6129. (h) Tomioka, J. *Ibid.* **1979**, *101*, 256–257; (i) Tomioka, H.; Inagaki, T.; Izawa, Y. *J. Chem. Soc., Chem. Commun.* **1976**, 1023–1024.

Chart I



moderate matrix isotope effects due to tunneling, but the relative magnitudes of the effects vary with the matrix. The anti form of the carbene must have a larger rate retardation than the syn form in 2-propanol-2-propanol- d_8 . The syn form must show a larger isotope effect in toluene-toluene- d_8 . One must conclude that even in cases of slow decay such as 2-propanol- d_8 and toluene- d_8 , the kinetics of 1-naphthylcarbene are far removed from the fast equilibrium conditions.

According to Scheme I it will be generally true that

$$\frac{-d[T_S]}{dt} = k_1[T_S] - k_2[T_A] + k_3[MH][T_S]$$

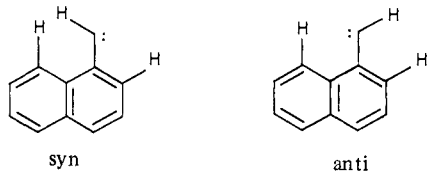
$$\frac{-d[T_A]}{dt} = k_2[T_A] - k_1[T_S] + k_4[MH][T_A]$$

As 1-naphthylcarbene is not at fast equilibrium in 2-propanol- d_8 and toluene- d_8 at 77 K, $k_3[MH]$ must be greater than, or comparable to, k_1 ; $k_3[MH] \gtrsim k_1$ (2-propanol- d_8 -toluene- d_8) and a similar relationship must hold for the anti form $k_4[MH] \gtrsim k_2$ (2-propanol- d_8 -toluene- d_8). This being the case, $k_3[MH] > k_1$ and $k_4[MH] > k_2$ in 2-propanol or toluene, as isotopic substitution of the matrix has a much larger effect on the bimolecular decay reaction than on syn-anti interconversion. As $k_3[MH]$ and $k_4[MH]$ are within a factor of 3 in 2-propanol or toluene at 77 K, $k_3[MH] > k_2$ and $k_4[MH] > k_1$ in 2-propanol and toluene. Therefore, $d[T_S]/dt = k_{syn}[T_S] > k_1[T_S]$ and $-d[T_A]/dt = k_{anti}[T_A] > k_2[T_A]$. The values of k_{syn} and k_{anti} can be obtained (albeit imprecisely) in units of s^{-1} by analyzing a small segment ($\sim 20\%$) of the decay over which a plot of $\log I$ vs. time is nearly linear. By choosing the first 20% of the decay (Table III) one obtains the maximum measured k_{syn} in s^{-1} . Therefore $k_1 < 1.5 \times 10^{-3} s^{-1}$ and $k_2 < 3.2 \times 10^{-3} s^{-1}$. From this data and the Arrhenius equation, the minimum barriers to interconversion (E_1 and E_2) can be calculated if the preexponential factor can be approximated. The solution $\log A$ value must be large, $\log A = 10-15 s^{-1}$, for movement of the carbenic hydrogen.²⁰ We will assume that the matrix does not depress the solution $\log A$ values because of the small size of the hydrogen atom. Solving the Arrhenius equation yields minimum barriers to carbene interconversion.

$$E_1(\text{syn} \rightarrow \text{anti}) > 4.5-6.3 \text{ kcal/mol}$$

$$E_2(\text{anti} \rightarrow \text{syn}) > 4.4-6.2 \text{ kcal/mol}$$

The π -electron systems of *syn*- and *anti*-1-naphthylcarbene are identical and thus equal in energy. If the σ electronic energies



of the two conformers are similar, the difference in energy of the two forms must be largely steric in origin. The *syn* conformer of 1-naphthylcarbene has an unfavorable steric interaction that is not present in the *anti* form. Hence *syn*-1 may be higher in energy than *anti*-1, $E_2 > E_1$ and $k_1 > k_2$. (See Chart I for energy diagram.)

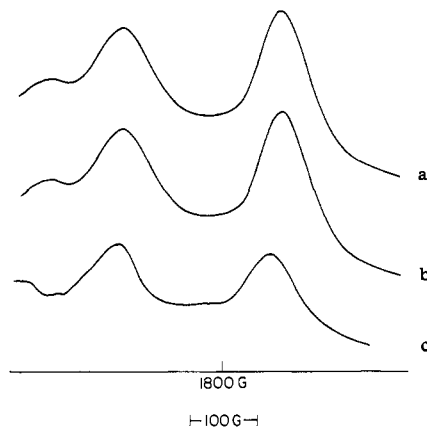


Figure 2. The D_{ZZ} transitions of the triplet *syn* (low field) and *anti* (high field) forms of 2-naphthylcarbene in (a) 2-propanol, (b) toluene, and (c) 2MTHF.

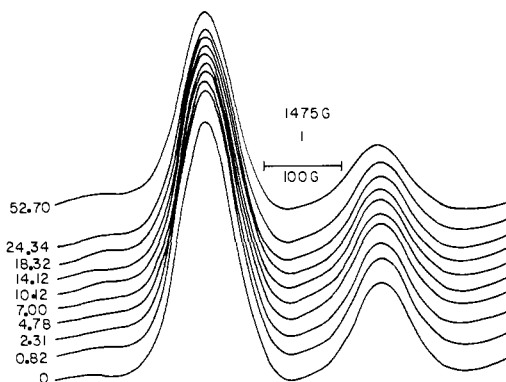
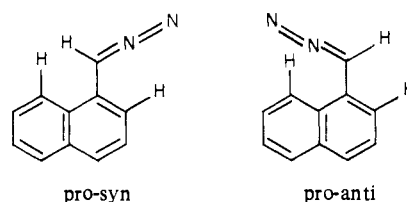


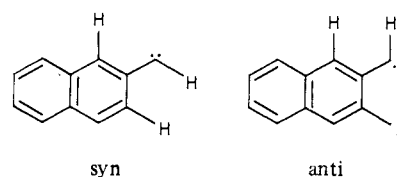
Figure 3. The time dependence of the triplet *syn* (low field) and *anti* (high field) D_{ZZ} transitions of 1-naphthyl- α - d -carbene in 2-propanol- d_8 . The time in minutes when the pen scans through the low-field maximum is listed.

Inspection of Figure 1 reveals that invariably $[T_S] > [T_A]$. This is further evidence against rapid syn-anti interconversion, as one predicts that $[T_A] > [T_S]$ at equilibrium on steric grounds. The relative concentrations of T_S and T_A probably reflects the initial populations of the diazo precursors. The identical steric argu-



ments predicts that the *pro-syn* diazo compound should be more prevalent than the *pro-anti* conformer. If photolysis of the diazo compound does not induce extensive syn-anti isomerization, then $[T_S]$ should indeed be greater than $[T_A]$.² This argument holds even if the diazo precursor is not in the same plane as the aromatic ring system, as long as it is not orthogonal to it.

The steric interactions in *syn*- and *anti*-2-naphthylcarbene are very similar. Hence, the relative populations of T_S and T_A should



be more similar for 2-naphthylcarbene than for the 1-naphthyl system. Accordingly, the energy content and rate constants of 2-naphthyl should be more evenly balanced than 1-naphthyl-

Table VII. Pseudo-First-Order Matrix Rate Constants for 9-Anthrylcarbene

matrix	temp, °C	k , $s^{-1/3}$	concn, M
2-PrOH	-196	0.026 ± 0.002	s^a
	-178	0.059 ± 0.004	s
	-174	0.063 ± 0.006	s
2-PrOH- d_8	-196	0.005	s
	-166	0.036 ± 0.003	s
	-162	0.057 ± 0.004	s
	-156	0.113 ± 0.008	s
2-PrOH- $O-d$	-174	0.061 ± 0.002	s
	-171	0.073 ± 0.004	s
	-168	0.087 ± 0.002	s
	-165	0.117 ± 0.008	s
toluene	-196	0.044 ± 0.004	0.116
	-169	0.129 ± 0.012	0.116
	-165	0.143 ± 0.016	0.116
2-PrOH-2- d	-174	0.053 ± 0.002	s
	-171	0.063 ± 0.004	s
	-168	0.075 ± 0.004	s
	-165	0.091 ± 0.006	s
	-155	0.143 ± 0.004	0.106
toluene- d_8	-196	0.008	0.106
	-161	0.079 ± 0.003	0.106
	-158	0.115 ± 0.006	0.106
	-155	0.143 ± 0.004	0.106

^a Saturated (<0.1 M).

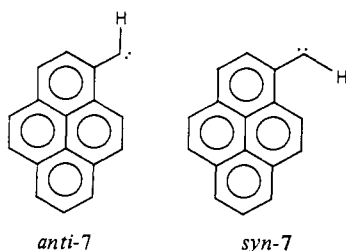
carbene. This reasoning is consistent with the observed facts. $[T_S]$ does not equal $[T_A]$ at 77 K in various matrices (Figure 2), but the distribution is not as lopsided as in 1-naphthylcarbene (Figure 1). In fact, the data of Table II indicate that at 77 K, $k_{syn} \approx k_{anti}$ for 2-naphthylcarbene in 2-propanol and toluene. This latter observation is consistent with fast equilibration kinetics but does not conclusively establish this condition.

Matrix isotope effects are particularly useful in distinguishing fast or slow equilibrium conditions in 2-naphthylcarbene. If fast equilibration conditions are realized, then isotopic substitution of the matrix should retard both k_{syn} and k_{anti} equally. The data of Table II show that on passing from 2-propanol to 2-propanol- d_8 , k_{syn} is retarded by 38%, while k_{anti} slows down by 58%. k_{syn}/k_{anti} changes from 0.93 to 1.38 upon isotopic substitution of the matrix. Similar results are obtained in the toluene-toluene- d_8 system, where k_{syn}/k_{anti} changes from 0.88 to 1.86. The matrix isotope effects show that it is fortuitous that $k_{syn} \approx k_{anti}$ for 2-naphthylcarbene and that fast equilibrium kinetics do not prevail in these systems at 77 K.

Following the reasoning for 1-naphthylcarbene, $k_{syn} > k_1$ and $k_{anti} > k_2$ for 2-naphthylcarbene in 2-propanol and toluene at 77 K, and $k_1 < 1.5 \times 10^{-3} s^{-1}$ and $k_2 < 1.8 \times 10^{-3} s^{-1}$. Assuming that $\log A$ is again between 10 and 15 s^{-1} and solving the Arrhenius equation, we obtain $E_1 > 4.5$ –6.3 kcal/mol and $E_2 > 4.5$ –6.3 kcal/mol.

9-Anthryl- and 2-Pyrylcarbene. 9-Anthrylcarbene **3** gives only one set of triplet resonance absorptions as both of its planar conformations are equivalent by symmetry. The decay of this carbene is much slower than **1** or **2** in 2-propanol or toluene at 77 K as shown in Tables VII and VIII. Isotopic substitution of 2-propanol and toluene led to dramatic increases in both the E_a and $\log A$ values. This requires that 9-anthrylcarbene is decaying by hydrogen atom abstraction from the solvent by quantum mechanical tunneling.

2-Pyrylcarbene **7** should have two distinct conformational isomers and give two sets of triplet ESR spectra. However, in

**Table VIII.** Matrix Arrhenius Parameters for Bimolecular Rate Decay of 9-Anthrylcarbene

matrix	$\log A$, $s^{-1/3} M$	E , cal/mol
2-PrOH	-0.52 ± 0.21	727 ± 112
2-PrOH- $O-d$	0.18 ± 0.35	1081 ± 158
2-PrOH-2- d	0.18 ± 0.14	1127 ± 74
2-PrOH- d_8	0.30 ± 0.30	1297 ± 128
toluene	-0.40 ± 0.18	701 ± 87
toluene- d_8	0.50 ± 0.27	1322 ± 127

Table IX. Pseudo-First-Order Decay Rate Constants for 2-Pyrylcarbene and Their Related Bimolecular Arrhenius Constants

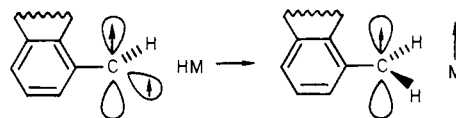
matrix	temp, °C	k , $s^{-1/3}$	concn, M
2-PrOH	-196	0.059 ± 0.004	s^a
	-182	0.089 ± 0.014	s
	-176	0.145 ± 0.008	s
$\log A = -0.55 \pm 0.15 M^{-1} s^{-1/3}$, $E = 605 \pm 66$ cal/mol			
2-PrOH- d_8	-196	0.020	s
	-175	0.085 ± 0.004	s
	-172	0.125 ± 0.004	s
	-169	0.184 ± 0.001	s
$\log A = 0.9 \pm 0.26 M^{-1} s^{-1/3}$, $E = 1284 \pm 134$ cal/mol			
toluene	-196	0.097 ± 0.001	0.113
	-184	0.171 ± 0.001	0.113
	-180	0.197 ± 0.007	0.113
$\log A = 0.20 \pm 0.12 M^{-1} s^{-1/3}$, $E = 686 \pm 69$ cal/mol			
toluene- d_8	-196	0.031 ± 0.002	0.134
	-180	0.084 ± 0.004	0.134
	-173	0.141 ± 0.001	0.134
$\log A = 0.63 \pm 0.23 M^{-1} s^{-1/3}$, $E = 1013 \pm 130$ cal/mol			

^a Saturated (<0.1 M).

2-propanol only a single set of resonances were observed ($D/hc = 0.40 \pm 0.01$ cm^{-1} , $E/hc = 0.019 \pm 0.002$ cm^{-1}). Zero field splitting calculations of Roth indicate that the $|D/hc|$ values of the 2-pyryl syn and anti carbene are very similar.⁸ The observed spectrum may be the unresolved combination of two conformational isomers, or it may be due to a single species. Carbene *syn-7* is the more likely carbene to be observed based on the steric preferences of the diazo precursor.

Isotopic substitution of the 2-propanol or toluene matrices containing 2-pyrylcarbene dramatically affects the Arrhenius parameters. The $\log A$ and E_a both increase upon isotopic substitution, analogous to the effects observed with other arylcarbenes (Table IX). The interpretation again is a hydrogen atom tunneling phenomenon.

The rate of a hydrogen atom tunneling process is dependent upon the barrier height and width.¹⁸ The barrier height will be relatively constant for **1**, **2**, **3**, and **7** if the migrating hydrogen atom trajectories are similar throughout the series. This is a consequence of the fact that it is the nonconjugated, in-plane carbene orbital that is abstracting hydrogen. This orbital, which contains an odd electron, resembles the highly reactive phenyl radical. (Ingold has shown that hindered phenyl radicals in-



tramolecularly abstract hydrogen in a tunneling process.²¹) The barrier width is simply the distance the hydrogen must tunnel from a matrix molecule MH to the arylcarbene. The barrier width

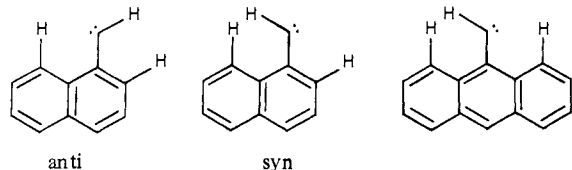
(21) Brunton, G.; Ariller, D.; Barclay, L. R. C.; Ingold, K. U. *J. Am. Chem. Soc.* **1976**, *98*, 6803–6811.

Table X. Pseudo-First-Order Decay Rate Constants of 1-Naphthyl-8-*d*-carbene and Their Related Bimolecular Arrhenius Parameters

matrix	temp, °C	$k_{\text{syn}}, \text{s}^{-1/3}$	$k_{\text{H}}/k_{\text{D}}$	$k_{\text{antib}}, \text{s}^{-1/3}$	$k_{\text{H}}/k_{\text{D}}$
2-PrOH	-196	0.101 ± 0.004	1.04	0.126 ± 0.001	1.4
	-182	0.216 ± 0.004			
	-179	0.248 ± 0.010			
$\log A = 0.28 \pm 0.18 \text{ M}^{-1} \text{ s}^{-1/3}, E = 803 \pm 70 \text{ cal/mol}$					
2-PrOH- <i>d</i> ₈	-196	0.028 ± 0.001	1.11	0.034 ± 0.001	1.18
	-179	0.101 ± 0.004		0.113 ± 0.006	
	-176	0.123 ± 0.002		0.129 ± 0.010	
$\log A = 0.62 \pm 0.26 \text{ M}^{-1} \text{ s}^{-1/3}, E = 1135 \pm 96 \text{ cal/mol (syn)}$; $\log A = 0.47 \pm 0.34 \text{ M}^{-1} \text{ s}^{-1/3}, E = 1030 \pm 97 \text{ cal/mol (anti)}$					
toluene ^a	-196	0.130 ± 0.003	0.98	0.134 ± 0.002	1.05
	-184	0.204 ± 0.002			
	-180	0.256 ± 0.030			
$\log A = 0.08 \pm 0.18 \text{ M}^{-1} \text{ s}^{-1/3}, E = 591 \pm 54 \text{ cal/mol}$					
toluene- <i>d</i> ₈ ^b	-196	0.055 ± 0.001	0.62	0.063 ± 0.001	
	-173	0.195 ± 0.009			
	-170	0.229 ± 0.003			
$\log A = 0.50 \pm 0.18 \text{ M}^{-1} \text{ s}^{-1/3}, E = 872 \pm 74 \text{ cal/mol}$					

^a Diazo concentration is 0.141 M. ^b Diazo concentration is 0.123 M.

varies, even within a single polycrystalline matrix. The ensemble of carbenes within a matrix is held rigidly in sites of differing environment, hence the nonexponential signal decay. It is not obvious why the reactivity of **1**, **2**, **3**, and **7** averaged over the different reactive sites (k_{obsd} in $\text{s}^{-1/3}$) varies in the manner observed. Models suggest that the carbene center of *syn*-1-naphthylcarbene should have a more accessible carbene center, hence a smaller barrier width and therefore higher reactivity. This is exactly contrary to experimental observation; *anti*-1-naphthyl is considerably more reactive than the *syn* form at 77 K.



The approach of a tunneling hydrogen atom to the carbene center of 9-anthrylcarbene or 2-pyrylcarbene appears very similar to the naphthalene example. However, the former case is 85% slower than *anti*-1-naphthylcarbene, whereas the latter example is virtually identical with it. The origin of the relative reactivities of **1**, **2**, **3**, and **7** may well reside in the microcrystalline environment of the respective carbenes. The decay reactions can derive from sites of different tunneling widths, complicating a simple comparison of relative reactivity of the various carbenes.

Carbene Isotope Effects. The effects of isotopic substitution of the carbene are not as straightforward as those of matrix substitution. Isotopic substitution of the naphthalene proton at the 8 (peri) position should affect the kinetics of the anti form much more than the *syn*. This is exactly what is observed in 2-propanol (Table X). With 2-propanol, the peri deuterium selectively decelerates the decay of the anti carbene. In 2-propanol-*d*₈ and toluene the isotope effects are small, the effect upon the anti carbene being only slightly larger than that of the *syn* conformer. The direction of the isotope effect is not obvious. One could easily have imagined that the lower zero-point vibrational amplitude of deuterium relative to hydrogen would have made the peri anti carbene site more sterically accessible and accelerated the reaction rate.

Deuteration of the carbene center produces some changes in the reaction rate constant. For 1-naphthyl- α -deuteriocarbene the anti rate constant is nearly half that of the unlabeled carbene in 2-propanol, but the *syn* α -deuteriocarbene reaction rate is retarded

by 24%. For the same carbene there is no appreciable isotope effect in 2-propanol-*d*₈ or toluene. The effect reappears modestly in *syn*-1-naphthyl- α -deuteriocarbene in toluene-*d*₈. For 2-naphthyl- α -deuteriocarbene the isotope effects are very similar for both the *syn* and anti forms. In 2-propanol $k_{\text{H}}/k_{\text{D}} = 0.56$ and 0.62, and in 2-propanol-*d*₈ $k_{\text{H}}/k_{\text{D}} = 0.85$ and 0.87 for the respective conformers. The carbene α -deuterio effects on the Arrhenius parameters are not outside of experimental error. The origin of these effects also remain uncertain, but may be related to subtle changes in the crystal packing of the protio and deuterio sites.

Conclusions

The absolute decay rates of the *syn* and anti forms of 1- and 2-naphthylcarbene, 9-anthrylcarbene, and 2-pyrylcarbene can be measured at low temperature by ESR. Matrix isotope effects reveal that the carbene decay is via pseudo-first-order hydrogen abstraction from the matrix. The signal decay is nonexponential due to site problems in the matrix but can be fitted to a $\log I$ vs. $t^{1/3}$ dependence. Isotopic substitution of the matrix reveals that hydrogen atoms migrate via quantum mechanical tunneling through a small barrier. The kinetics of the *syn* and anti forms of 1- and 2-naphthylcarbene indicate that the rate of *syn*-anti interconversion is much slower than the rate of carbene reaction with the matrix. The activation barrier to *syn*-anti interconversion for 1- and 2-naphthylcarbene must exceed 4.5–6.3 kcal/mol.

Experimental Section

1- and 2-naphthyl-diazomethane and 9-anthryldiazomethane were prepared by literature procedures.²² 2-Propanol and toluene were purified by distillation and storage over molecular sieves. All of the deuterated solvents were purchased from Merck (>98% isotopic purity) and used without further purification. Samples were prepared by weight and syringed into 4-mm quartz ESR tubes. They were vacuum sealed by using three freeze-thaw cycles.

Temperature control was carried out by employing a variable-temperature control accessory attached with the instrument. All temperatures above -196 °C were obtained by passing regulated amounts of N₂ gas through the cavity. The N₂ gas was precooled by passing through liquid nitrogen. The exact temperature of the probe was measured by inserting an Omega digital thermometer into the cavity before and after each kinetic run. The data was analyzed only when there had been no temperature drift. The thermometer had an accuracy of ± 0.5 °C. The temperature can be kept constant for several hours. The irradiation was passed through Schoeffel infrared filters to reduce sample heating. For kinetics at liquid nitrogen temperature, the sample tube was placed in a Dewar containing liquid nitrogen.

Pseudo-first-order kinetics were followed by observing the decay of the signal intensity of the D_{zz} transition of the triplet. The transition can be conveniently recorded and the time at which the pen crosses the peak maximum noted (Figure 3). The base line is drawn and the height of the peak maximum from the base line is used as a measure of the intensity and concentration of the triplet carbene at that time. The carbene peak shape does not change over the course of the decay reaction. In all of the kinetic runs the signal was recorded up to 50–85% of decay, from which the rate constants were calculated by plotting $\log [\text{intensity}]$ vs. $t^{1/3}$.

General Preparation of Labeled Diazo Compounds. 1. From *p*-Toluenesulfonylhydrazones. Approximately 0.1 g of *p*-toluenesulfonylhydrazone is dissolved in 25 mL of freshly dried and distilled THF in a three necked flask fitted with a septum and kept under nitrogen. The flask is cooled with a dry ice-acetone bath for 30 min and then 1 equiv of a *n*-butyllithium solution in hexane (Aldrich) is added via syringe. The solution is allowed to warm to room temperature and then briefly heated on a steam bath until the color turns orange or red. After the solution is cooled to room temperature, the solvent is removed under vacuum. The residue is extracted into hexane, dried over sodium sulfate, and filtered, and the solvent is removed, leaving the desired diazo compound. The diazo compound can be stored indefinitely in liquid nitrogen until needed.

2. From Hydrazones. Hydrazone, yellow mercuric oxide, and anhydrous sodium sulfate in molar ratio of 1:2:0.5 were vigorously stirred in ethyl ether. One or two drops of saturated ethanolic potassium hydroxide was added to the solution. After 30 min the solution was filtered and the solvent removed on a rotoevaporator. The residue was extracted

Table XI. Pseudo-First-Order Decay Rate Constants of 1-Naphthylcarbene- α -*d*

matrix	temp, °C	$k_{\text{syn}}, \text{s}^{-1/3}$	$k_{\text{H}}/k_{\text{D}}$	$k_{\text{anti}}, \text{s}^{-1/3}$	$k_{\text{H}}/k_{\text{D}}$	concn, M
2-PrOH	-196	0.085 ± 0.002	1.24	0.087 ± 0.010	1.98	s^a
	-185	0.117 ± 0.010				s
	-182	0.137 ± 0.010				s
2-PrOH- d_8	-196	0.032 ± 0.003	0.97	0.038 ± 0.003	1.06	s
	-179	0.075 ± 0.008				s
	-176	0.105 ± 0.008				s
	-173	0.119 ± 0.006				s
	-196	0.119 ± 0.008				s
toluene	-196	0.119 ± 0.008	1.07	0.147 ± 0.012	0.96	0.14
	-185	0.184 ± 0.012				0.14
toluene- d_8	-196	0.036 ± 0.003	0.94	0.057 ± 0.004	0.78	0.16
	-180	0.059 ± 0.006				0.16
	-176	0.109 ± 0.008				0.216 ± 0.020

^a Saturated (<0.1 M).Table XII. Arrhenius Parameters for the Bimolecular Decay of 1-Naphthylcarbene- α -*d*

	syn		anti	
	$\log A, \text{s}^{-1/3} \text{M}^{-1}$	E, cal	$\log A, \text{s}^{-1/3} \text{M}^{-1}$	$E, \text{cal/mol}$
2-PrOH	-0.55 ± 0.30	550 ± 124		
2-PrOH- d_8	-0.12 ± 0.24	829 ± 85	-0.32 ± 0.29	751 ± 89
toluene	-0.25 ± 0.28	594 ± 104		
toluene- d_8	-0.15 ± 0.32	828 ± 134	-0.22 ± 0.27	875 ± 113

into pentane. Removal of the pentane yields the desired diazo compound. In some cases it is possible to recrystallize the diazo compound from cold pentane.

8-Deuterio-1-naphthoic Acid. Five grams of 8-bromo-1-naphthoic acid was dissolved in 50 mL of D_2O containing 5 mL of 40% sodium deuterioxide (Aldrich). To this was added 100 mg of 10% palladium on carbon. This solution was treated with 30 psi of deuterium gas. Gas (2 psi) was absorbed within 30 min. There was no further absorption of gas within the next 24 h. After the excess deuterium gas was flushed out, the solution was filtered and neutralized with 85% D_3PO_4 (Merck). The precipitated 8-deuterio-1-naphthoic acid was collected, washed with D_2O , and then dried in vacuo overnight. The yield obtained was 3.5 g, mp 160.5–161 °C. Mass spectral analysis showed 12% d_0 , 77% d_1 , and 12% d_2 , and no starting material was present. Carbon-13 NMR of 1-naphthoic acid showed all 10 aryl resonances, only one of which (at 125.4 ppm) disappeared in the deuterated sample.

8-Deuterio-1-naphthalenemethanol. A 3.4-g sample of 8-deuterio-1-naphthoic acid in 250 mL of THF was added to 1.7 g of LiAlH_4 in 50 mL of THF. The solution was refluxed overnight, cooled to room temperature, quenched with 2-propanol, then water, then 2-N NaOH. The solution was poured into a separatory funnel containing 300 mL of ether. The ether phase was washed with water, dried over MgSO_4 , and filtered, and the solvent was removed, leaving an oil which crystallized on standing; yield 2.8 g. Mass spectral analysis revealed 90% d_1 and 10% d_0 . Carbon-13 NMR showed 10 aryl resonances in 1-naphthalenemethanol, one of which (δ 123.6) disappeared in the deuterated sample.

8-Deuterio-1-naphthaldehyde. A 1.5-g sample of 8-deuterio-1-naphthalenemethanol and 10 mL of D_2O were added to a suspension of 15 g of MnO_2 in 500 mL of toluene which had been previously activated by azeotropic distillation. The solution was connected to a Dean Stark trap and azeotropically refluxed for 12 h. The solution was filtered hot, the solvent removed, and the residual oil vacuum distilled [103–105 °C (1.0 mm)]; yield 0.6 g. Mass spectral analysis revealed 97% d_1 and 3% d_0 . Proton NMR of the product showed that the 8 H multiplet of δ 9.1 had disappeared. Carbon-13 NMR analysis of 1-naphthaldehyde showed nine aryl resonances. 8-Deuterio-1-naphthaldehyde also showed nine aryl resonances, but the peak at δ 124.8 was reduced in intensity by roughly 50%.

8-Deuterio-1-naphthaldehyde *p*-Toluenesulfonylhydrazone. 8-Deuterio-1-naphthaldehyde (0.32 g) and 0.3 g of *p*-toluenesulfonylhydrazone were dissolved in 15 mL of ethanol-*O-d*. The alcohol was

distilled under nitrogen until the volume of solution was 3 mL. After the solution was cooled to room temperature, D_2O was added dropwise until the solution turned cloudy. The solution was cooled to -20 °C, whereupon the product precipitated. The product was collected, air-dried, and then dried under vacuum for 1 h. The yield obtained was 0.6 g, mp 130–132 °C. Proton NMR of the undeuterated material showed that the 8 H multiplet overlapped the $\text{N}=\text{C}-\text{H}$ singlet at δ 8.6. In the deuterated compound the 8 H multiplet and the NH absorption disappeared. Carbon-13 NMR of the undeuterated material showed 14 aryl peaks. The deuterated material showed 13 peaks, the peak at δ 124 having disappeared. Mass spectral analysis revealed 2% d_0 , 49% d_1 , and 49% d_2 .

8-Deuterio-1-naphthylidiazomethane. The 8-deuterio-1-naphthaldehyde *p*-toluenesulfonylhydrazone was treated with *n*-butyllithium according to the general procedure described. The NMR of the unlabeled diazo compound reveals that the 8 H multiplet is not distinctive. Hence although IR and NMR demonstrate that the desired diazo compound was formed, the extent of deuteration was not determined.

2-Naphthalene- α,α -dideuteriomethanol. A 10-g sample of 2-naphthoic acid in 250 mL of THF was added to 3 g of LiAlD_4 (Merck, >99.9%) in 50 mL of THF. The solution was refluxed overnight, cooled to room temperature, and then quenched with 2-propanol, then water, then 2 M H_2SO_4 . The solution was stirred 30 min and then poured into ether. The aqueous phase was discarded, and the ether phase was washed 3 times with 2 N NaOH, dried over MgSO_4 , and filtered, and the solvent was removed, leaving a white crystalline residue; yield, 9 g; mp 74.5–76.5 °C. Mass spectroscopy was too complex for exact isotopic analysis. Proton NMR showed >98% deuterium incorporation.

2-Naphth- α -deuterioaldehyde. Eight grams of 2-naphthalene- α,α -dideuteriomethanol was added to a solution of 25 g of MnO_2 which had been previously activated by azeotropic reflux in 500 mL of toluene. The solution was connected to a Dean Stark trap and azeotropically refluxed for 1 h. It was filtered hot and the solvent was removed. The residual white crystals were recrystallized from ethanol-water to give 7.2 g of product in two crops, mp 53–54 °C. Mass spectral analysis revealed virtually 100% d_1 . Proton NMR showed the aldehyde C-H resonance at δ 10.1 had disappeared completely.

2-Naphth- α -deuterioaldehyde *p*-Toluenesulfonylhydrazone. 2-Naphthaldehyde- α -*d* (1.6 g) and 1.9 g of *p*-toluenesulfonylhydrazone were dissolved in 50 mL of absolute ethanol. This solution was concentrated to 10 mL by boiling on a hot plate. Upon cooling the solution to -20 °C, the product precipitated (mp 171–175 °C). NMR analysis does not yield the extent of deuteration as the $\text{H}-\text{C}=\text{N}-\text{N}$ proton cannot be resolved from the aromatic multiplets.

2-Naphthyl- α -deuteriodiazomethane. The 2-naphth- α -deuterioaldehyde *p*-toluenesulfonylhydrazone (0.1 g) was treated with *n*-butyllithium according to the general procedure described. NMR analysis indicates that the $\text{H}-\text{C}=\text{N}=\text{N}$ proton at δ 4.9 has disappeared completely.

2-Pyrenecarboxaldehyde *p*-Toluenesulfonylhydrazone. 2-Pyrenecarboxaldehyde (2.3 g) and 1.9 g of *p*-toluenesulfonylhydrazone were dissolved in 50 mL of THF. To this was added 100 mL of absolute ethanol. The solution was concentrated to 50 mL by boiling on a hot

Table XIII. Pseudo-First-Order Decay Rate Constants of 2-Naphthylcarbene- α -*d* at 77 K

matrix	$k_{\text{syn}}, \text{s}^{-1/3}$	$k_{\text{H}}/k_{\text{D}}$	$k_{\text{anti}}, \text{s}^{-1/3}$	$k_{\text{H}}/k_{\text{D}}$	concn, M
2-PrOH	0.103 ± 0.004	0.56	0.099 ± 0.004	0.62	s^a
2-PrOH- d_8	0.040 ± 0.004	0.88	0.030 ± 0.001	0.87	s
toluene	0.212 ± 0.022	0.48	0.214 ± 0.012	0.54	0.143
toluene- d_8	0.121 ± 0.006	0.45	0.083 ± 0.006	0.36	0.112

^a Saturated (<0.1 M).

plate. When the solution is cooled to $-20\text{ }^{\circ}\text{C}$, a dark-green glass formed, and later yellow crystals. The yellow precipitate was collected, washed with cold ethanol, and then vacuum dried. The yield obtained was 1.6 g, mp $185\text{--}186\text{ }^{\circ}\text{C}$ with bubbling (the crystals turned red at $160\text{ }^{\circ}\text{C}$).

2-Pyryldiazomethane. 2-Pyrenecarboxaldehyde *p*-toluenesulfonylhydrazone was treated with *n*-butyllithium according to the general procedure described. Infrared analysis of the product solid showed diazo absorption at 2070 cm^{-1} .

1-Naphthalene- α,α -dideuteriomethanol. Ten grams of 1-naphthoyl chloride in 200 mL of ether was added to 2.8 g of LiAlD_4 (Merck, >99.9%) in 150 mL ether. The addition was so regulated as to maintain a gentle reflux. The solution was stirred 12 h and then quenched with 2-propanol, then H_2O , then 150 mL of 30% aqueous KOH. The ether phase was separated, washed with water, dried over MgSO_4 , and rotovapped to dryness. The residual oil crystallized on standing. It was recrystallized from ethanol-water to give 1.2 g of product, mp $62\text{--}63\text{ }^{\circ}\text{C}$. Mass spectral and proton NMR analysis showed >99% d_2 .

1-Naphth- α -deuterioaldehyde. A 7-g sample of 1-naphthalene- α,α -dideuteriomethanol was added to a suspension of 30 g of MnO_2 in 500 mL of toluene which had been previously activated by azeotropic reflux for 12 h. The solution was filtered hot, and the solvent was removed,

leaving 6.2 g of clear oil. NMR showed no aldehydic C-H. The infrared showed no C-H stretch at 2735 and 2840 but strong C-D at 2070 and 2120 cm^{-1} .

1-Naphth- α -deuterioaldehyde Hydrazone. A 1.1-g sample of 1-naphth- α -deuterioaldehyde was dissolved in 30 mL of absolute alcohol. To this was added 0.7 g of 97% hydrazine. The solution was concentrated to a volume of 7 mL by boiling on a hot plate. When the solution was cooled to $-20\text{ }^{\circ}\text{C}$, the product precipitated. It was collected and air-dried, mp $83\text{--}88\text{ }^{\circ}\text{C}$. The mass spectrum showed >99% d_1 . NMR analysis reveals that the H-C=N-N resonance at $\delta\ 8.3$ had disappeared completely.

1-Naphthyl- α -deuteriodiazomethane. 1-Naphth- α -deuterioaldehyde hydrazone was oxidized with HgO according to the general procedure described. NMR analysis reveals that the H-C=N=N- resonance at $\delta\ 5.4$ had disappeared completely.

Acknowledgment. We gratefully acknowledge support of this work by the National Science Foundation (Grant No. CH-7900896). The authors thank Professors Hine and McCurdy for valuable discussions.

Magnetic Studies and the Crystal and Molecular Structure of $[\text{enH}_2][\text{V}(\text{hedta-H})]_2\cdot 2\text{H}_2\text{O}$: A Novel Di- μ -alcoxy-Bridged Dimer of Seven-Coordinate V(III)

Rex E. Shepherd,*^{1a} William E. Hatfield,*² Debashis Ghosh,^{1b} C. David Stout,^{1b} Frank J. Kristine,^{1a} and J. R. Ruble^{1b}

Contribution from the Department of Chemistry and the Department of Crystallography, University of Pittsburgh, Pittsburgh, Pennsylvania 15260, and the Department of Chemistry, University of North Carolina at Chapel Hill, Chapel Hill, North Carolina 27514.

Received January 5, 1981. Revised Manuscript Received April 24, 1981

Abstract: The crystal and molecular structure of $[\text{enH}_2][\text{V}(\text{hedta-H})]_2\cdot 2\text{H}_2\text{O}$ has been determined from 2734 independent reflections (Mo $K\alpha$ radiation) to $R = 0.042$ ($R_w = 0.035$). The structure displays novel bridging of the two V atoms by the alcoxy groups formed by deprotonation of the *N*-hydroxyethyl functionality of the parent hedta^{3-} ligand [$\text{hedta}^{3-} = N$ -hydroxyethylethylenediaminetriacetate anion]. Each V(III) center in the dimer has sevenfold coordination which is approximated by a slightly distorted pentagonal bipyramid. The central angles of the alcoxy-bridged V_2O_2 core are virtually strain-free angles: V-O-V angles are 108° ; O-V-O angles are 72° . The V-V separation is 3.296 \AA . The magnetic susceptibilities of the $[\text{enH}_2][\text{V}(\text{hedta-H})]_2\cdot 2\text{H}_2\text{O}$ salt were determined from 4.24 to 91.4 K by the vibrating magnetometer method. The susceptibilities are consistent with a spin-only interaction of two d^2 centers described by the Hamiltonian, $-2J\mathbf{S}_1\cdot\mathbf{S}_2$. The best fit parameters for the susceptibility data are $g = 1.93$ and $-2J = 17.1\text{ cm}^{-1}$. The $2J$ value is consistent with the dialcoxy-bridging unit of the V_2O_2 core. The formation of the dialcoxy-bridged unit of the V(III) dimer in $[\text{V}(\text{hedta-H})]_2^{2-}$ appears to account for the kinetically slow intramolecular electron-transfer reaction with $\text{V}^{\text{II}}\text{OV}^{\text{IV}}(\text{hedta})_2^{2-}$.

Although the mechanistic aspects of the formation of the binuclear complex containing V(III) centers chelated by the hedta ligand have been studied,³ it remained uncertain whether the V(III) centers are joined by an oxo ligand as in the Fe(III) complex, $[\text{Fe}(\text{hedta})]_2\text{O}^{2-}$, or by dihydroxy-bridging ligands or by some other coordination arrangement. The binuclear complex, V(III, III), of this report is produced from monomeric $\text{V}^{\text{III}}(\text{hedta})$ by two paths: (1) by combination of two molecules of $\text{V}(\text{hedta})(\text{OH})^-$ or $\text{V}(\text{hedta})(\text{OH})^-$ and $\text{V}(\text{hedta})(\text{H}_2\text{O})^3$ or (2) by a novel redox reaction.^{4,5} The cross reaction between $\text{VO}(\text{hedta})^-$

and $\text{V}(\text{hedta})^-$ produces the V(III, III) binuclear complex by two paths: (a) by intramolecular electron transfer within a $\text{V}^{\text{II}}\text{V}^{\text{IV}}\text{O}(\text{hedta})_2^{2-}$ intermediate which is detectable on the stopped-flow time scale and (b) by combination of $\text{V}(\text{hedta})$ monomer species formed during the competitive outer-sphere electron-transfer path. On the basis of the solvent-exchange rate of V(II), the enhancement provided for solvent exchange with hedta^{3-} coordination on V(II), and the substitution-inert vanadyl oxygen in $\text{VO}(\text{hedta})^-$, it has been concluded that the unusually intense spectral features of the $\text{V}^{\text{II}}\text{V}^{\text{IV}}\text{O}(\text{hedta})_2^{2-}$ species, which differ from the less intense spectral parameters of the V(III, III) complex, originate in oxo bridging between V(II) and V(IV) in the cross reaction.^{4,5} Although the V(II, IV) intermediate has a short lifetime of about 25 ms, this lifetime is actually unusually long

(1) (a) Department of Chemistry, University of Pittsburgh. (b) Department of Crystallography, University of Pittsburgh.

(2) Department of Chemistry, University of North Carolina at Chapel Hill.

(3) Kristine, F. J.; Shepherd, R. E. *J. Am. Chem. Soc.* **1977**, *99*, 6562.

(4) Kristine, F. J.; Shepherd, R. E. *J. Chem. Soc., Chem. Commun.* **1976**, 994.

(5) Kristine, F. J.; Shepherd, R. E. *J. Am. Chem. Soc.* **1978**, *100*, 4398.